Published in final edited form as:
Vision Res. 2007 December ; 47(26): 3259–3268.

Macular pigment, photopigments, and melanin: distributions in young subjects determined by four-wavelength reflectometry

Richard A. Bone, **Betty Brener**, and **Jorge C. Gibert**
Department of Physics, Florida International University, 11200 SW 8th Street, Miami, FL 33199, USA

Abstract

We have developed an objective procedure, using a modified retinal camera, to determine macular pigment (MP) optical density distributions in the human retina. Using two multi-band filters, reflectance maps of the retinas of young subjects (<25 years old) were obtained at 460, 528, 610 and 670 nm, without pupil dilation. The log-transformed maps were combined linearly to yield optical density maps of MP, cone and rod photopigments, and melanin. MP optical density and heterochromatic flicker photometry results for 22 subjects were in reasonable agreement. Cone photopigments, like MP, showed similar, well-defined peaks at the fovea, whereas rod photopigment showed a minimum. Melanin was more broadly distributed.

Keywords

macular pigment; reflectometry; retinal camera; lutein; zeaxanthin

Introduction

The risk of age-related macular degeneration (AMD) depends on a number of factors including those that appear to be linked to photooxidative stress (Beatty, Koh, Phil, Henson & Boulton, 2000). Many studies suggest that macular pigment (MP) may reduce photooxidative stress by blocking blue light and through antioxidant action (Kim, Nakanishi, Itagaki & Sparrow, 2006, Snodderly, 1995). On the other hand, no differences in MP optical density were found in eyes with and without age-related maculopathy in a cross-sectional study (Berendschot, Willemse-Assink, Bastiaanse, deJong & Van Norren, 2002), nor did MP appear to be protective against early AMD in a longitudinal study (Kanis, Berendschot & Van Norren, 2006). Both studies involved participants from the Rotterdam Study. Nevertheless, the potential importance of macular pigment to the health of the eye has prompted the development of several methods for measuring its density in the retina. The list of methods includes heterochromatic flicker photometry (HFP) (Beatty, Koh, Carden & Murray, 2000, Bone & Landrum, 2004a, Snodderly, Mares, Wooten, Oxton, Gruber & Ficek, 2004, Wooten, Hammond Jr., Land & Snodderly, 1999), which is probably the most widely used method, and minimum motion photometry (Moreland, 2004). Both of these are psychophysical procedures and require active participation by the subject. Others, that are physical methods and require relatively passive participation by the subject, are based on resonance Raman spectroscopy (Bernstein, Zhao, Wintch, Ermakov, McClane & Gellermann, 2002, Neelam, O'Gorman, Nolan, O'Donovan, Wong, Au

Corresponding author: Richard A. Bone, Tel: +1 305 348 3082; fax: +1 305 348 6700, E-mail address: bone@fiu.edu.

Eong & Beatty, 2005), lipofuscin autofluorescence (Delori, Goger, Hammond Jr., Snodderly & Burns, 2001, Wüstemeyer, Moessner, Jahn & Wolf, 2003), and retinal reflectometry (Kilbride, Alexander, Fishman & Fishman, 1989, Van de Kraats, Berendschot & Valen, 2006, Van de Kraats, Berendschot & Van Norren, 1996).

The optical density spectrum of the MP may be obtained from measurements of foveal and peripheral reflectance spectra, a technique that was first introduced by Brindley and Willmer (Brindley & Willmer, 1952). They ascribed the difference between foveal and peripheral reflectance primarily to the presence of MP in the foveal region. Later investigators improved the reflectance measurements to account for the effects of non-uniform distributions of other pigments in the light path as well as light-scattering in the ocular media. To remove the effects of melanin (present in the RPE and choroid) and oxyhemoglobin (present in the vascular choroid) from the MP optical density spectrum, they developed curve-fitting procedures to model the contribution from each pigment (Delori & Pflibsen, 1989, Van de Kraats et al., 1996, Van Norren & Tiemeijer, 1986). Based on what is perhaps the most highly detailed model, Van de Kraats et al. have developed an instrument to provide fast assessment of central MP density (Van de Kraats et al., 2006). The model takes into account absorption by multiple chromophores, scattering and reflection by different layers and the influence of the Stiles-Crawford effect. With some simplifications, the model contains 7 free parameters whose values are adjusted to produce a match with a full reflectance spectrum from 400 to 800 nm.

A further development, imaging reflectometry, was introduced by Kilbride et al. in order to generate two-dimensional MP optical density distributions in the retina (Kilbride et al., 1989). With a modified retinal camera, they captured digital images of the bleached retina at a number of wavelengths including 462 nm (peak MP optical density) and 559 nm (zero MP optical density). Bleaching reduces the effects of light absorption by photopigments that would vary with retinal location. A simple procedure would have been to equate the difference between the log-transformed (and aligned) 462 and 559 nm images to the MP (double) optical density distribution at 462 nm, in accordance with the Brindley and Willmer model. However, they first weighted the 559 nm image by a factor representing the ratio of extinction coefficients of combined hemoglobin and melanin at the two wavelengths. In so doing, they attempted to remove their effects from the MP optical density distribution. However, inaccuracies could arise if the relative contributions of melanin and hemoglobin varied across the retina. A similar technique was used by Chen et al. to study the variation of the MP distribution with age (Chen, Chang & Wu, 2001). Bour et al. used imaging reflectometry (480 and 540 nm) combined with the simple Brindley and Willmer model to study MP distributions in children (Bour, Koo, Delori, Apkarian & Fulton, 2002). A complication, which a digital camera would have eliminated, was their use of a film camera with the additional step of scanning the developed film in order to digitize the images. Several studies describe the adaptation of the scanning laser ophthalmoscope (SLO), a relatively expensive instrument, for imaging reflectometry (Berendschot, Goldbohm, Klöpping, van de Kraats, van Norel & van Norren, 2000, Elsner, Burns, Beausencourt & Weiter, 1998, Elsner, Moraes, Beausencourt, Remky, Burns, Weiter, Walker, Wing, Raskauskas & Kelley, 2000, Wüstemeyer, Moessner, Jahn, Nestler, Barth & Wolf, 2002). The superior SLO images are far less prone to scattered light from the ocular media than those captured with a fundus camera. Typically, images of the retina, usually in a bleached state, are captured at the argon laser wavelengths, 488 and 514 nm. Digital subtraction of the log-transformed images is assumed to provide the MP (double) optical density. As in the study of Bour et al., it is assumed that optical density differences across the retina for pigments other than MP are negligible. In a highly simplified version of imaging reflectometry, a single image of the retina is captured under blue light at a wavelength at which the MP absorbs strongly. It is assumed that the decreased intensity seen in the foveal part of the image is due only to the presence of MP. The technique has been used in conjunction with an SLO to study the effects of lutein supplementation (Schweitzer, Lang, Beuermann, Remsch, Hammer &

Thamm, 2002), and in conjunction with a fundus camera to study MP in albinos (Abadi & Cox, 1992). With the single image technique, it is not possible to factor in the effects of non-uniform distributions of other pigments

Here we describe a novel adaptation of imaging reflectometry that employs a standard, non-mydriatic, digital retinal camera and does not require photopigment bleaching. As such, the method has the advantage of being accessible to vision scientists in non-clinical settings who are not permitted to dilate their subjects' pupils. Without bleaching, the distributions of rod and cone photopigments in the retina must be taken into consideration. Also taken into account is the distribution of melanin, which is different in the RPE and choroid. Our goal has been to develop an objective procedure for measuring MP optical density that is based on commonly available equipment and is simple, fast and relatively inexpensive. An added benefit of the method is its ability to generate simultaneously optical density distributions of photopigments and melanin.

Methods

Model

Our method for acquiring MP optical density distributions is based on a simplified model of the human retina shown in Fig. 1. Light incident at an arbitrary point on the retina, and subsequently remitted by means of reflection and scattering, is assumed, in general, to undergo absorption by the ocular media, MP, cone and rod photopigments, hemoglobin, and melanin. The model is similar to "Model I" of Delori and Pflibsen (Delori et al., 1989). Some of the light is specularly reflected at the inner limiting membrane, for example giving rise to the foveal reflex that is particularly apparent in young subjects. It is also possible that the majority of remitted light from the deeper retinal layers undergoes multiple scattering in the choroid rather than simply reflection by the sclera (Preece & Claridge, 2002). Depending on the proportions of light that are reflected and scattered, the model may provide an incorrect estimate of the total melanin. Our method compares the remitted light from different points on the retina. We assume that the absorption by the ocular media and choroidal hemoglobin produce uniform attenuation of light across the central retina (~15°) where our measurements are made, but that MP, cone photopigments, rod photopigment, and melanin have non-uniform distributions. We also avoid regions of the retinal image where specular reflections and blood vessels are apparent. Thus our model is represented by the absorbing layers shown in Fig. 1.

Limiting the model to four adjustable parameters, representing the four pigment optical density distributions, was dictated by the experimental procedure that involved relative reflectance measurements at four discrete wavelengths (see below). In other non-imaging methods, where absolute spectral reflectance is measured over a wide range of wavelengths, it is possible to incorporate many more free parameters into a model. Such parameters include scattering in the post-receptor layers and lens, reflections from the receptor disks and/or retinal pigmented epithelium, reflection from the inner limiting membrane, the Stiles-Crawford effect, as well as absorption by the ocular media, hemoglobin and the four chromophores in our model (Delori et al., 1989, Van de Kraats et al., 2006, Van de Kraats et al., 1996). We are not aware of the existence of technology with which it is currently possible to combine retinal imaging with full spectral reflectance measurements. Therefore, with images available at only a few, discrete wavelengths, a decision must be made to limit the number of free parameters that a model contains. Our choice of melanin, cone photopigments, and rod photopigment, in addition to MP, was largely driven by the realization that all of these pigments have significant spatial variation across the retina.

A simplification in our model is the representation of the cone and rod photopigments as two absorbers in series. This was the representation adopted by Kilbride and Keehan in their

assessment of visual pigments by imaging fundus reflectometry (Kilbride & Keehan, 1990). The alternative configuration of two side-by-side absorbers would introduce an intractable problem to our model. It may also not be completely appropriate. Histological sections through the retina often show imperfect alignment of rods and cones (Enoch, 1981). A photon entering a photoreceptor obliquely may escape somewhere along the outer segment and be absorbed instead by an adjacent photoreceptor (Walraven & Bouman, 1960). Van der Kraats et al. found that, in order to account for the average retinal reflectance spectrum in 10 subjects, the fraction of light escaping from the outer segment was ~ 81% (Van de Kraats et al., 1996). The results of Chen and Makous showed that half or more of the light entering near the edge of the pupil was absorbed by cones other than those on which it originally fell (Chen & Makous, 1989). Furthermore, our model describes a double-pass through each absorbing layer. Thus light passing through a cone on the first pass could pass through a rod on the return pass, and vice versa. Therefore neither the series nor side-by-side configuration is truly representative of the state of affairs in the retina and a better representation may be some combination of the two. Part of the justification for adopting the series configuration in our model is that it leads not only to a tractable system, but also to plausible distributions of cone and rod photopigments.

Because we have four unknown pigment distributions in the model, we need to obtain images of the retina at a minimum of four wavelengths. Provided we know how the extinction coefficient of each pigment varies with wavelength, the four images can be combined to yield the relative optical density distribution for each pigment. For example, if light of wavelength λ is incident at a point in the fovea (*F*), and is of intensity $I_{F,\lambda}$, the F remitted intensity is $I_{F,\lambda}T^2_{MP,F,\lambda}T^2_{ME,F,\lambda}T^2_{CP,F,\lambda}T^2_{RP,F,\lambda}R_{F,\lambda}$. The additional subscripts refer to macular pigment (*MP*), melanin (*ME*), cone photopigment (*CP*), and rod photopigment (*RP*). *T* is the transmittance of an absorbing pigment and $R_{F,\lambda}$ is the effective reflectance of the sclera/choroidal layer. A similar expression would apply to a point in the extra-fovea(*E*). The logarithm (to base 10) of the ratio of the remitted intensity in the fovea to that in the extra-fovea is given by

$$L_\lambda = \log\left(\frac{I_{F,\lambda}R_{F,\lambda}}{I_{E,\lambda}R_{E,\lambda}}\right) - 2(D_{MP,F,\lambda} + D_{ME,F,\lambda} + D_{CP,F,\lambda} + D_{RP,F,\lambda} - D_{MP,E,\lambda} - D_{ME,E,\lambda} - D_{CP,E,\lambda} - D_{RP,E,\lambda})$$

where $D(=-\log T)$ is the optical density of an absorbing pigment. We assume that the incident intensity and the reflectance are the same at the foveal and extra-foveal locations so the first term on the right is zero. Therefore

$$L_\lambda = -2\{(D_{MP,F,\lambda} - D_{MP,E,\lambda}) + (D_{ME,F,\lambda} - D_{ME,E,\lambda}) + (D_{CP,F,\lambda} - D_{CP,E,\lambda}) + (D_{RP,F,\lambda} - D_{RP,E,\lambda})\} \quad (1)$$

For each of four different wavelengths, we write an equation like equation 1. Prior to solving these as simultaneous equations, we must convert all optical densities to their values at one of the four wavelengths. For this we used the spectral data of Hunold and Malessa for melanin (Hunold & Malessa, 1974), Bone *et al.* for MP (Bone, Landrum & Cains, 1992), DeMarco *et al.* for cone photopigments (DeMarco, Pokorny & Smith, 1992), and Crescitelli and Dartnall for rod photopigment (Crescitelli & Dartnall, 1953). For the cones, we assumed a long- to medium-wavelength-sensitive ratio of 1.8:1, based on an average of estimates in the literature ranging from 1.46 to 2.36 (Cicerone & Nerger, 1989, Van de Kraats et al., 1996, Vos & Walraven, 1970). Like van de Kraats et al., we ignored the presence of the sparsely distributed short-wavelength-sensitive cones (Van de Kraats et al., 1996). The four wavelengths that we selected were 460 (blue, *B*), 528 (green, *G*), 610 (red, *R*), and 670 nm (far red, *FR*). The solutions of the equations yield the following optical density differences (fovea - extra-fovea) at 460 nm:

$$D_{MP,F,B} - D_{MP,E,B} = -0.538L_B + 0.535L_G - 1.26L_R + 1.88L_{FR} \quad (2)$$

$$D_{CP,F,B} - D_{CP,E,B} = -0.402 L_R + 0.555 L_{FR} \quad (3)$$

$$D_{RP,F,B} - D_{RP,E,B} = 0.0383 L_B - 0.535 L_G + 1.66 L_R - 1.38 L_{FR} \quad (4)$$

$$D_{ME,F,B} - D_{ME,E,B} = -1.05 L_{FR} \quad (5)$$

In the case of macular pigment, it is possible to choose an extra-foveal location, e.g. at an eccentricity of ~ 7° or greater, at which the MPOD may be assumed to be negligible. Equation 2 then yields the absolute MPOD at any location, such as the peak value at the center of the fovea.

Experimental setup

Retinal images were acquired with a Topcon TRC NW5SF non-mydriatic retinal camera (Topcon, Paramus NJ) equipped with a Sony DXC970MD video camera. This type of camera employs three CCD chips and a system of prisms and color filters that split the image and provide each chip with an appropriate spectral response. The responses appear as the broad bandwidth curves in Fig. 2. The retinal camera was modified by replacing the exciter filter (used in fluorescein angiography) between the flash-lamp and the subject's eye with either of two filters (Omega Optical, Brattleboro VT). The first was a triple-bandpass interference filter with peak transmittances at 460, 528, and 610 nm, each transmitting band being ~ 20 nm wide. The filter was designed so that each transmission band would overlap with only one of the three CCD response curves, as shown in Fig. 2. The complex spectral shape of each band is a typical feature of multi-bandpass filters and might be expected to influence the measurements. However, the optical density variation of any of the four chromophores in our model is small over wavelength ranges that characterize the fine features in the transmission bands, so the complexity of the band shape is probably immaterial. The second filter was a double-bandpass filter with peak transmittances at 535 and 670 nm. The 670 nm band, also ~ 20 nm wide, together with those of the other filter, provided the four wavelengths needed by the model. The 535 nm band was not used in the model; rather it ensured that retinal blood vessels were clearly defined in the resulting image and could therefore be used as an aid to image alignment.

The camera was set to capture 20° diameter images. Features that would affect the linearity of the camera's response, such as gamma and white balance, were turned off via the on-screen menu. The linearity was checked for each color channel by capturing images of a series of certified reflectance standards (Labsphere, North Sutton NH) illuminated by the camera's flash lamp. The overall gain, red channel gain, and blue channel gain were set at 12, −30, and 25 dB respectively. These settings were found to produce mid-level responses in the three color channels without saturation. Images were transferred to a computer using a FlashBus MV Pro frame grabber (Integral Technologies, Inc., Indianapolis, IN) and stored in TIF format. Image analysis was performed using ImagePro Plus software (MediaCybernetics, Silver Spring MD).

HFP was conducted using an instrument and procedure that have been described elsewhere (Bone et al., 2004a). Briefly, subjects viewed a 1.5°, ~ 4000 Td stimulus that alternated in wavelength between 460 and 540 nm. The 460 nm test wavelength was provided by an interference filter of ~ 20 nm bandwidth, i.e. the same width as the filter transmission bands used with the camera. The stimulus was viewed at 0° and 8° eccentricity and the intensity of the 460 nm component was adjusted in each case to produce a flicker null. The subject's MP optical density at 460 nm was determined as the log ratio of intensity settings.

Subjects

22 subjects with ages from 18 to 24 years were recruited from the student population of Florida International University. Informed consent, approved by the University's Institutional Review

Board, was obtained from each subject after the nature of the study had been explained. The study conformed to the tenets of the Declaration of Helsinki. Subjects received training in HFP and were enrolled in the study once their MP optical density measurements were accompanied by a standard error in the mean that was consistently ≤ 0.020 absorbance units.

Experimental procedure

The subject was seated in front of the retinal camera in a darkened laboratory that promoted pupil dilation. (While the camera is non-mydriatic, a minimum pupil diameter of 4 mm is specified.) Forehead and chin rests were provided to help maintain head position. Focusing and alignment were achieved under infra-red illumination to prevent pupil constriction. The subject was instructed to fixate on the mid-point of the focusing bars that were visible through the camera lens. Images were captured using each of the two filters that were described earlier. The double-band filter was used first as this resulted in less pupil constriction that could otherwise decrease the retinal illumination when capturing the second image. During the same session, the subject's MP optical density was determined by HFP. Each subject attended 6 to 8 such sessions at ~ 2 week intervals in order to assess the repeatability of reflectometry in comparison with HFP.

As a test of the validity of our model, we measured the optical density distributions of MP, cone and rod photopigments, and melanin in one eye of a dark-adapted subject, and in the same eye after a period of photopigment bleaching (~ 5.5 log photopic trolands for ~ 3 min).

Image analysis

The two captured images were processed by an ImagePro Plus macro that was written to perform the following operations: 1) The two images were automatically aligned with each other, the triple-band filter image acting as the anchor. 2) Eight-bit gray scale images were extracted from the "red," "green," and "blue" channels of the color image obtained with the triple-band filter. An 8-bit gray scale image was extracted from the "red" channel of the aligned color image obtained with the double-band filter. 3) The four gray scale images were converted from fixed to floating point representation in order to preserve information. 4) The resulting images were transformed logarithmically. (This procedure results in very low pixel values; hence the need for floating point representation.) 5) The logarithmically transformed images were combined linearly according to equations 2 – 5. This procedure resulted in gray scale images that revealed through their pixel values the relative optical density distributions of MP, cone and rod photopigments, and melanin at 460 nm. 6) The images for the cones and rods were multiplied by appropriate factors so that they represented the relative optical density distributions at the peak wavelengths respectively (550 nm for cones, 505 nm for rods).

Horizontal line-scans through the foveal region of each image were obtained and the data, i.e. the pixel values along the line, were transferred to a graphing program, SigmaPlot (Systat Software Inc., Richmond CA), in order to run a smoothing routine. Peak pigment optical density was determined by measuring the peak height above the baseline of the distribution.

Results

Sample images showing the spatial distributions of the relative optical densities of MP, cone and rod photopigments, and melanin for one of the subjects are shown in Fig. 3. The optical densities represent approximate averages over a ~ 20 nm wavelength range (the width of the filter transmission bands) centered on 460 nm for MP and melanin, 550 nm for cone photopigments, and 505 nm for rod photopigments. As noted earlier, the fine features in the spectral profile of each transmitting band would be expected to have a negligible effect on these optical density distributions. The foveal region in the images is intentionally below center.

Images produced with this camera system typically have a small, lighter region in the center that is presumably an artifact of the optics. For illustrative purposes only, the images in Fig. 3 have been enhanced by adjusting brightness, contrast and gamma. Since relative optical density is given by the pixel value, lighter regions in the images represent higher optical densities. Thus MP and cone photopigments are seen to peak sharply in the fovea, rod photopigments dip to minimum in this region, and melanin is more broadly distributed. Fig. 4 illustrates the corresponding optical density distributions of the pigments, after smoothing, along horizontal lines through the fovea. It should be noted that the photopigments are readily bleached by light and regenerate in the dark. Thus the optical density values merely reflect the state of affairs at the time of image capture, specifically when using the triple-band filter. (The 670 nm band of the double-band filter is negligibly absorbed by the rod and cone photopigments, and provides information only on melanin which does absorb at this wavelength. Information on photopigments is provided only by the triple-band filter.)

For the single subject for whom measurements were compared in the dark-adapted and bleached states, MP and melanin distributions were not significantly affected by the state. On the other hand, the cone peak optical density decreased from 0.46 in the dark-adapted state to 0.16 in the bleached state. Similarly the valley in the rod photopigment distribution went from a depth of 0.29 (dark adapted) to a depth of 0.09 (bleached). Because of the variability in the optical density of cone and rod photopigments based on their degree of bleach, we did not look for possible correlations between these optical densities and that of the photostable MP. We did, however, investigate whether there might be a correlation between MP and the other photostable pigment, melanin, but found none.

Since our major concern is MP, distributions of this pigment for a number of subjects are shown in Fig. 5a. The plots illustrate the variability not only in peak height, but also peak width, and are typical of about 45% of the subjects. For the remaining 55% of the subjects, subsidiary maxima or shoulders at ~ ± 0.7° eccentricity were observed, consistent with the ringlike structures that others have seen in MP distributions (Berendschot & Van Norren, 2006,Delori, Goger, Keilhauer, Salvetti & Staurenghi, 2006). Samples are shown in Fig. 5b. The fluctuations that occur in the plots between ~ 2 and 5° eccentricity are associated with bright areas, often ring-shaped, often sharp-edged, that frequently appeared in the original retinal images. They have the appearance of areas of specular reflection. During image processing, these artifacts propagate and are visible in the final pigment optical density distributions. (Note the dark rings clearly visible in Fig. 3a and b.) Thus we do not believe that the corresponding fluctuations in Fig. 5 represent fluctuations in MP optical density, but are merely artifacts. Generally, the correlation between left and right eye measurements was high ($r^2 = 0.53$, $p = 0.0001$ for peak height), as illustrated in Fig. 6. A comparison between the peak values, relative to baseline, for all 22 subjects, and their MP optical density values obtained by HFP, is shown graphically in Fig. 7. These values represent the averages for each subject's left and right eye measurements obtained by each method.

Discussion

With only minor modification of a standard retinal camera, we have devised a rapid, objective method of determining not only a subject's peak MP optical density, but also the complete, 2-dimensional MP optical density distribution in the central ~ 15° of the retina. Compared with HFP, the new reflectometry method is rapid. Images for one eye, using the triple- and double-band filters, could be acquired in less than one minute. Processing time to produce the images shown in Fig. 3 added another ~ 10 seconds to the procedure. By comparison, a testing period of about 10 minutes per eye in a trained subject was needed to obtain MP optical density by HFP. In terms of reproducibility, the methods were very comparable. The standard deviation of a set of measurements in the same eye was typically 0.05 absorbance units or less for either

reflectometry or HFP. An additional advantage of the reflectometry method is the simultaneous generation of corresponding distributions of cone and rod photopigments and melanin. The model on which the method is based, which is certainly a simplification of the retina's reflectance properties, is strengthened by the plausibility of these distributions. For example, the MP distributions of Fig. 5 are very similar to those that were obtained by similar (Berendschot et al., 2006,Kilbride et al., 1989), as well as unrelated, techniques (Berendschot et al., 2006,Delori et al., 2006,Hammond Jr., Wooten & Snodderly, 1997,Sharifzadeh, Bernstein & Gellerman, 2006). The method is clearly capable of revealing the ringlike features of the MP that we and others (Berendschot et al., 2006,Delori et al., 2006) have observed in over half the subjects studied. The range of peak MP optical densities is consistent with those reported when using HFP (Hammond & Caruso-Avery, 2000,Rodriguez-Carmona, Kvansakul, Harlow, Köpcke, Schalch & Barbur, 2006,Snodderly et al., 2004). Also the MP distribution in the retina has been reported to be very similar to that of the cone photopigments (Elsner et al., 1998), and this is borne out by a comparison of the distributions shown in Figs. 4a and 4b. The similarity is to be expected since the majority of the MP resides in the Henle fibers – the photoreceptor axons (Snodderly, Auron & Delori, 1984), and in the foveal region the photoreceptor population is dominated by cones. Our rod photopigment distributions (Fig. 4c) are consistent with the distribution of rods themselves, which are missing from the foveal center but rise in number to a broad, maximum density at about 17 to 20° from the center (Osterberg, 1935). They are also very similar to those obtained by Tornow and Stilling who employed imaging densitometry with a scanning laser ophthalmoscope to measure rod photopigment distributions (Tornow & Stilling, 1998), and by Kilbride and Keehan who, like us, used a modified fundus camera (Kilbride et al., 1990). Finally, the choroidal melanin distribution is characterized by a broad maximum in the fovea whereas the RPE melanin distribution tends to be generally more uniform and of lower optical density, though with a small, narrow peak in the fovea (Weiter, Delori, Wing & Fitch, 1986). Some combination of these characteristics would certainly not be inconsistent with the type of distribution exemplified in Fig. 4d.

The validity of our model is also strengthened by the appropriate responses of the pigment distributions when the subject's eye was exposed to a bleaching light. It would appear from the results that approximately 2/3 of the cone and rod photopigments were bleached. The level of bleaching is probably attributable to the time taken for the subject to change the position of her eye from the bleaching equipment to the camera, and for the camera operator to bring the retina into focus.

HFP is often used as a yardstick relative to which other methods of measuring MP optical density are compared. A justification for this view is that when the HFP test wavelength is varied in order to determine MP optical density as a function of wavelength, the resulting spectrum duplicates that obtained *in vitro* using appropriate mixtures of lutein and zeaxanthin (Bone et al., 1992, Wooten & Hammond Jr., 2005). Thus we were interested in comparing HFP with our new method. The data presented in Fig. 7 reveal a reasonably high linear correlation ($r^2 = 0.62$, $p < 0.0001$), but the fitted line does not have the desired slope of 1.0 that would indicate complete agreement between the two methods. Others too have found less than perfect correlations between MP optical density measurements by reflectometry and HFP. Values of r^2 of 0.38 (Delori et al., 2001) and 0.31 (Van de Kraats et al., 2006) have been reported. However, possible agreement between two methods of measuring a parameter cannot be assessed by the correlation coefficient. A far more informative procedure is to generate a Bland-Altman plot of the difference in measurements by the two methods (y axis) versus the mean of the measurements (x axis) (Bland & Altman, 1986). This is shown for our data in Fig. 8. The mean difference between the methods can be seen to be very close to zero and within the 95% confidence interval (− 0.039 to + 0.032 AU). All of the differences are essentially within ± 2SD (equal to ± 0.16 AU) of the mean, the so-called "limits of agreement." Compared with HFP, there appears to be a tendency for reflectometry to give a higher MP optical density for

the subjects with low optical density, but this may simply be a consequence of the small sample size.

The discrepancies between the results of HFP and reflectometry could be due to a number of factors affecting the reliability of either method. A fundamental assumption of HFP is that the relative sensitivity of the retina to the test and reference wavelengths is, in the absence of MP, the same at the foveal and parafoveal locations that are used for testing. Recent work in our lab indicates that this assumption may be invalid possibly due to a subject-dependent, lower long- to medium-wavelength-sensitive cone ratio (LWS/MWS) in the fovea compared with the parafovea (Bone, Landrum, Adams & Gibert, 2007). In addition, photopigment self-screening could differentially affect measurements made at these two locations (Werner, Bieber & Schefrin, 2000). There is also some disagreement over which characteristic of the MP optical density distribution is determined by HFP. Our own work has indicated that, rather than providing the average optical density over the stimulated area, HFP provides the value at an eccentricity that is approximately 50% of the stimulus radius (Bone, Landrum & Gibert, 2004b). There is another school of thought that supports the “edge hypothesis,” maintaining that what is measured is the optical density at the stimulus edge (Delori et al., 2001, Hammond Jr. et al., 1997, Snodderly et al., 2004, Werner et al., 2000).

In the case of our new reflectometry method, with its 4 free parameters, a number of simplifications were necessary in order to make the procedure viable. Thus the rods and cones were treated as two sequential absorbers, rather than side-by-side absorbers, and the cone layer was assumed to be comprised of LWS and MWS photoreceptors that maintained a constant ratio (1.8:1) across the retina. We investigated the effects of altering this ratio from a low of 1:1 to a high of 2:1 and found no measurable change in any of the four chromophore’s optical density distribution. Short-wavelength-sensitive (SWS) cones were omitted because their numbers, relative to LWS and MWS cones are known to vary across the retina, and this would have added more parameters to the model that our procedure would have been unable to handle. However, SWS cones are relatively sparse in the retina, comprising ~ 7% of all cones within 4 mm of the foveal center (Curcio, Allen, Sloan, Lerea, Hurley, Klock & Milam, 1991), so it is possible that their contribution to the overall optical density of the cone layer may justifiably be ignored. We also had to omit a potentially more significant factor, intra-ocular light scatter, which is known to increase with age, but is also quite variable at any given age (Westheimer & Liang, 1995). The majority of scattered light reaching the camera would be due to backscattering of the incident flash by the lens of the eye. The result would be a decrease in the contrast of the image and a resulting under-estimate of the MP optical density. Additional stray light can arise from reflection at the inner limiting membrane. Delori and Pflibsen noted a significant increase in the estimate of MP optical density when a small, inner limiting membrane reflectance was introduced to their model (Delori et al., 1989). It has been argued that the scattered light problem underlies an observed decrease in MP optical density with age when determined by the Raman method (Hammond Jr., Wooten & Smollon, 2005). In order to minimize this potential source of error, we restricted our study population to those less than 25 years old whose intra-ocular media would be relatively clear. On the other hand, younger subjects are more prone to stronger reflections from the inner limiting membrane, leading to a pronounced foveal reflex. Where this was a problem, we removed the affected pixel values from the line-scans prior to running the smoothing routine that produced the distributions of Figs 4 and 5. Another possible source of unwanted light reaching the camera would be any fluorescent chromophores in the light path. In principle, these could be excited by the shorter wavelengths that are transmitted through the filters and the resulting fluorescence detected by the longer wavelength channels in the camera. Finally, the effective absorbance spectrum of melanin in the RPE/choroid is not well known and a number of estimates have been published (Gabel, Birngruber & Hillekamp, 1978, Geeraets, Williams, Chan, Ham Jr., Guerry III & Schmidt, 1962, Hunold et al., 1974, Menon, Persad, Haberman, Kurian & Basu, 1982). An

additional problem is that the melanin layers are both absorbers and scatterers and, as such, cannot readily be incorporated into our model. The absorbance spectrum for melanin of Hunold et al., that we used in our model, is considerably flatter than that, for example, of Gabel et al. The ratio of absorbances at 460 and 670 nm is ~ 2.1 for Hunold et al. and ~ 4.8 for Gabel et al. We found a sizeable but variable reduction, averaging about 20%, in our peak MP optical densities when using the spectrum of Gabel et al. Our decision to use that of Hunold et al. was based on the improved agreement that we obtained with the HFP data.

In conclusion, we have developed a novel procedure, based on reflectometry, which provides a rapid determination of the optical density distributions of a number of absorbing pigments in the eye, principally the MP. The method is non-invasive, does not require pupil dilation and is accessible to anyone with a digital retinal camera. We are currently investigating its suitability for use with older subjects who may have significant lenticular light scatter.

Acknowledgements

Support provided by NIH grants S06 GM08205 and R25 GM61347

References

Abadi R, Cox M. The distribution of macular pigment in human albinos. Invest Ophthalmol Vis Sci 1992;33:494–497. [PubMed: 1544776]

Beatty S, Koh HH, Carden D, Murray IJ. Macular pigment optical density measurement: a novel compact instrument. Ophthalmic Physiol Opt 2000;20:105–111. [PubMed: 10829132]

Beatty S, Koh H, Phil M, Henson D, Boulton M. The role of oxidative stress in the pathogenesis of age-related macular degeneration. Surv Ophthalmol 2000;45:115–134. [PubMed: 11033038]

Berendschot TTJM, Goldbohm RA, Klöpping WAA, van de Kraats J, van Norel J, van Norren D. Influence of Lutein Supplementation on Macular Pigment, Assessed with Two Objective Techniques. Invest Ophthalmol Vis Sci 2000;41:3322–3326. [PubMed: 11006220]

Berendschot TTJM, Van Norren D. Macular pigment shows ringlike structures. Invest Ophthalmol Vis Sci 2006;47:709–714. [PubMed: 16431971]

Berendschot TTJM, Willemse-Assink J, Bastiaanse M, deJong P, Van Norren D. Macular pigment and melanin in age-related maculopathy in a general population. Invest Ophthalmol Vis Sci 2002;43:1928–1932. [PubMed: 12037001]

Bernstein P, Zhao DY, Wintch S, Ermakov I, McClane R, Gellermann W. Resonance Raman measurement of macular carotenoids in normal subjects and in age-related macular degeneration patients. Ophthalmology 2002;109:1780–1787. [PubMed: 12359594]

Bland J, Altman D. Statistical methods for assessing agreement between two methods of clinical measurement. Lancet 1986;i:307–310. [PubMed: 2868172]

Bone RA, Landrum JT. Heterochromatic flicker photometry. Arch Biochem Biophys 2004a;430:137–142. [PubMed: 15369810]

Bone RA, Landrum JT, Adams M, Gibert JC. Validity of macular pigment optical density measurements by heterochromatic flicker photometry. Invest Ophthalmol Vis Sci 2007;48(ARVO EAbstract):2131.

Bone RA, Landrum JT, Cains A. Optical Density Spectra of the Macular Pigment in vivo and in vitro. Vision Res 1992;32:105–110. [PubMed: 1502795]

Bone RA, Landrum JT, Gibert JC. Macular pigment and the edge hypothesis of flicker photometry. Vision Res 2004b;44:3045–3051. [PubMed: 15474577]

Bour LJ, Koo L, Delori FC, Apkarian P, Fulton AB. Fundus photography for measurement of macular pigment density distribution in children. Invest Ophthalmol Vis Sci 2002;43:1450–1455. [PubMed: 11980860]

Brindley GS, Willmer EN. The reflexion of light from the macular and peripheral fundus oculi in man. J Physiol (Lond) 1952;116:350–356. [PubMed: 14939183]

Chen B, Makous W. Light capture by human cones. J Physiol (Lond) 1989;414:89–109. [PubMed: 2607444]

Chen SJ, Chang YC, Wu JC. The spatial distribution of macular pigment in humans. Curr Eye Res 2001;23:422–434. [PubMed: 12045892]

Cicerone C, Nerger J. The relative numbers of long-wavelength-sensitive to middle-wavelength-sensitive cones in the human fovea centralis. Vision Res 1989;29:115–128. [PubMed: 2773329]

Crescitelli F, Dartnall HJA. Human visual purple. Nature 1953;172:195–197. [PubMed: 13087150]

Curcio CA, Allen KA, Sloan KR, Lerea CL, Hurley JB, Klock IB, Milam AH. Distribution and morphology of human cone photoreceptors stained with anti-blue opsin. J Comp Neurol 1991;312:610–624. [PubMed: 1722224]

Delori FC, Goger DG, Hammond BR Jr, Snodderly DM, Burns SA. Macular pigment density measured by autofluorescence spectrometry: comparison with reflectometry and heterochromatic flicker photometry. J Opt Soc Am A 2001;18:1212–1230.

Delori FC, Goger DG, Keilhauer C, Salvetti P, Staurenghi G. Bimodal spatial distribution of macular pigment: evidence for a gender relationship. J Opt Soc Am A 2006;23:521–538.

Delori FC, Pflibsen KP. Spectral reflectance of the human ocular fundus. Appl Opt 1989;28:1061–1077.

DeMarco P, Pokorny J, Smith VC. Full-spectrum cone sensitivity functions for X-chromosome-linked anomalous trichromats. J Opt Soc Am 1992;9:1465–1476.

Elsner AE, Burns SA, Beausencourt E, Weiter JJ. Foveal cone photopigment distribution: small alterations associated with macular pigment distribution. Invest Ophthalmol Vis Sci 1998;39:2394–2404. [PubMed: 9804148]

Elsner AE, Moraes L, Beausencourt E, Remky A, Burns S, Weiter JJ, Walker J, Wing GL, Raskauskas P, Kelley L. Scanning laser reflectometry of retinal and subretinal tissues. Optics Express 2000;13:243–250.

Enoch, JM. Retinal receptor orientation and photoreceptor optics. In: Enoch, JM.; Tobey, FL., Jr, editors. Vertebrate Photoreceptor Optics. Berlin: Springer-Verlag; 1981.

Gabel, VP.; Birngruber, R.; Hillekamp, F. Visible and near infrared light absorption in pigment epithelium and choroid. In: Shimizu, K., editor. XXIII Concilium Ophthalmologicum (Excerpta Medica). Amsterdam: Elsevier; 1978.

Geeraets WJ, Williams RC, Chan G, Ham WT Jr, Guerry D III, Schmidt FH. The relative absorption of thermal energy in retina and choroid. Invest Ophthalmol Vis Sci 1962;1:340–347.

Hammond BR, Caruso-Avery M. Macular pigment optical density in a Southwestern sample. Invest Ophthalmol Vis Sci 2000;41:1492–1497. [PubMed: 10798668]

Hammond BR Jr, Wooten BR, Smollon B. Assessment of the validity of *in vivo* methods of measuring human macular pigment optical density. Optom Vis Sci 2005;82:387–404. [PubMed: 15894915]

Hammond BR Jr, Wooten BR, Snodderly DM. Individual variations in the spatial profile of human macular pigment. J Opt Soc Am A 1997;14:1–10.

Hunold W, Malessa P. Spectrophotometric determination of the melanin pigmentation of the human ocular fundus *in vivo.* Ophthalmic Res 1974;6:355–362.

Kanis M, Berendschot TTJM, Van Norren D. Influence of macular pigment and melanin on incident early AMD in a white population. Graefe's Arch Clin Exp Ophthalmol 2006;245:767–773.

Kilbride PE, Alexander KR, Fishman M, Fishman GA. Human macular pigment assessed by imaging fundus reflectometry. Vision Res 1989;29:663–674. [PubMed: 2626823]

Kilbride PE, Keehan K. Visual pigments in the human macula assessed by imaging fundus reflectometry. Appl Opt 1990;29:1427–1435.

Kim SR, Nakanishi K, Itagaki Y, Sparrow JR. Photooxidation of A2-PE, a photoreceptor outer segment fluorophore, and protection by lutein and zeaxanthin. Exp Eye Res 2006;82:828–839. [PubMed: 16364293]

Menon IA, Persad S, Haberman HF, Kurian CJ, Basu PK. A qualitative study of the melanins from blue and brown human eyes. Exp Eye Res 1982;34:531–537. [PubMed: 7075710]

Moreland JD. Macular pigment assessment by motion photometry. Arch Biochem Biophys 2004;430:143–148. [PubMed: 15369811]

Neelam K, O'Gorman N, Nolan J, O'Donovan O, Wong H, Au Eong K, Beatty S. Measurement of macular pigment: Raman spectroscopy versus heterochromatic flicker photometry. Invest Ophthalmol Vis Sci 2005;46:1023–1032. [PubMed: 15728561]

Osterberg G. Topography of the layer of rods and cones in the human retina. Acta Ophthalmol 1935;6 (Suppl):1–103.

Preece SJ, Claridge E. Monte Carlo modelling of the spectral reflectance of the human eye. Phys Med Biol 2002;47:2863–2877. [PubMed: 12222851]

Rodriguez-Carmona M, Kvansakul J, Harlow JA, Köpcke W, Schalch W, Barbur JL. The effects of supplementation with lutein and/or zeaxanthin on human macular pigment density and colour vision. Ophthalmic Physiol Opt 2006;26:137–147. [PubMed: 16460314]

Schweitzer D, Lang GE, Beuermann B, Remsch H, Hammer M, Thamm E. Objektive Bestimmung der optischen Dichte von Xanthophyll nach Supplementation von Lutein. Ophthalmologe 2002;99:270–275. [PubMed: 12058502]

Sharifzadeh M, Bernstein PS, Gellerman W. Nonmydriatic fluorescence-based quantitative imaging of human macular pigment distributions. J Opt Soc Am A 2006;23:2373–2387.

Snodderly DM. Evidence for protection against age-related macular degeneration by carotenoids and antioxidant vitamins. Am J Clin Nutr 1995;62(Suppl):1448S–1461S. [PubMed: 7495246]

Snodderly DM, Auron JD, Delori FC. The Macular Pigment. II Spatial Distribution in Primate Retinas. Invest Ophthalmol Vis Sci 1984;25:674–685. [PubMed: 6724837]

Snodderly DM, Mares JA, Wooten BR, Oxton L, Gruber M, Ficek T. Macular pigment measurements by heterochromatic flicker photometry in older subjects: the carotenoids and age-related eye disease study. Invest Ophthalmol Vis Sci 2004;45:531–538. [PubMed: 14744895]

Tornow RP, Stilling R. Variation in sensitivity, absorption and density of the central rod distribution with eccentricity. Acta Anat (Basel) 1998;162:163–168. [PubMed: 9831764]

Van de Kraats J, Berendschot TTJM, Valen S. Fast assessment of the central macular pigment density with natural pupil using the macular pigment reflectometer. J Biomed Opt 2006;11:064031. [PubMed: 17212554]

Van de Kraats J, Berendschot TTJM, Van Norren D. The pathways of light measured in fundus reflectometry. Vision Res 1996;36:2229–2247. [PubMed: 8776488]

Van Norren D, Tiemeijer LF. Spectral reflectance of the human eye. Vision Res 1986;26:313–320. [PubMed: 3716223]

Vos J, Walraven P. On the derivation of the foveal receptor primaries. Vision Res 1970;11:799–818. [PubMed: 5094974]

Walraven P, Bouman M. Relation between the directional sensitivity and spectral response curves in human cone vision. J Opt Soc Am 1960;50:780–784. [PubMed: 13842659]

Weiter JJ, Delori FC, Wing GL, Fitch KA. Retinal pigment epithelial lipofuscin and melanin and choroidal melanin in human eyes. Invest Ophthalmol Vis Sci 1986;27:145–152. [PubMed: 3943941]

Werner JS, Bieber ML, Schefrin BE. Senescence of foveal and parafoveal cone sensitivities and their relations to macular pigment density. J Opt Soc Am A 2000;17:1918–1932.

Westheimer G, Liang J. Influence of ocular light scatter on the eye's optical performance. J Opt Soc Am A 1995;12:1417–1424.

Wooten BR, Hammond BR Jr. Spectral absorbance and spatial distribution of macular pigment using heterochromatic flicker photometry. Optom Vis Sci 2005;82:378–386. [PubMed: 15894914]

Wooten BR, Hammond BR Jr, Land R, Snodderly D. A practical method for measuring macular pigment optical density. Invest Ophthalmol Vis Sci 1999;40:2481–2489. [PubMed: 10509640]

Wüstemeyer H, Moessner A, Jahn C, Nestler A, Barth T, Wolf S. A new instrument for the quantification of macular pigment density: first results in patients with AMD and healthy subjects. Graefe's Arch Clin Exp Ophthalmol 2002;240:666–671.

Wüstemeyer H, Moessner A, Jahn C, Wolf S. Macular pigment density in healthy subjects quantified with a modified confocal scanning laser ophthalmoscope. Graefe's Arch Clin Exp Ophthalmol 2003;241:647–651.

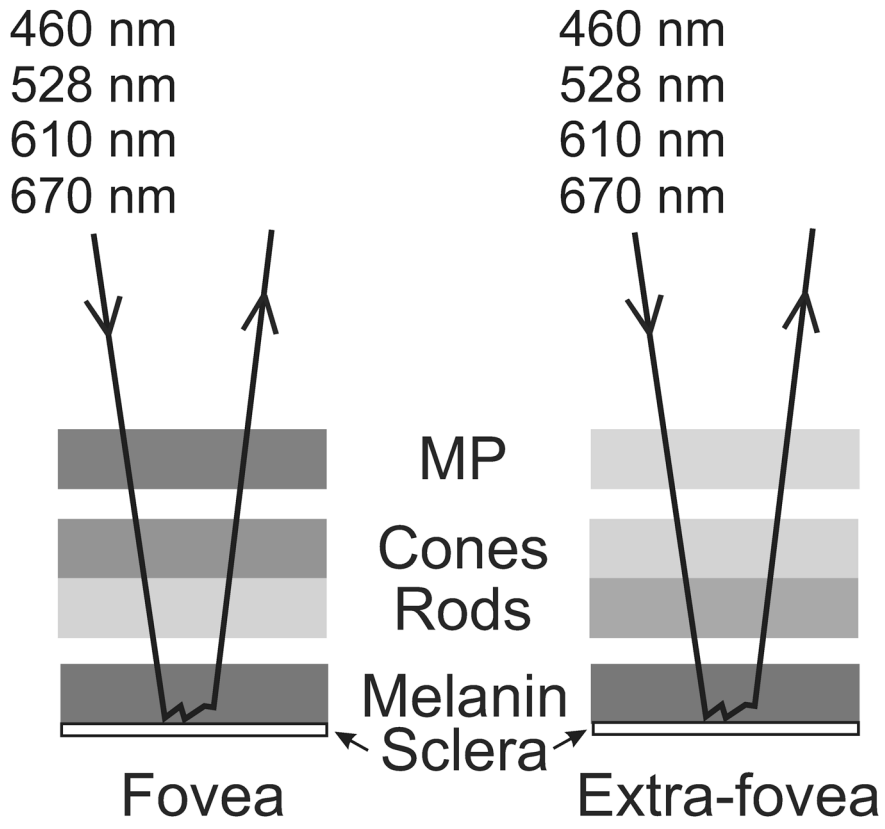

Fig. 1.

Model of the retina as a sequence of absorbing layers: macular pigment (MP), cone and rod photopigments, and melanin. Incident light, of each of four wavelengths, is absorbed to a greater or lesser extent by each layer and the amount each layer absorbs is generally different depending on retinal location. The light is returned through the layers after multiple scattering in the melanin layer and/or reflection at the sclera.

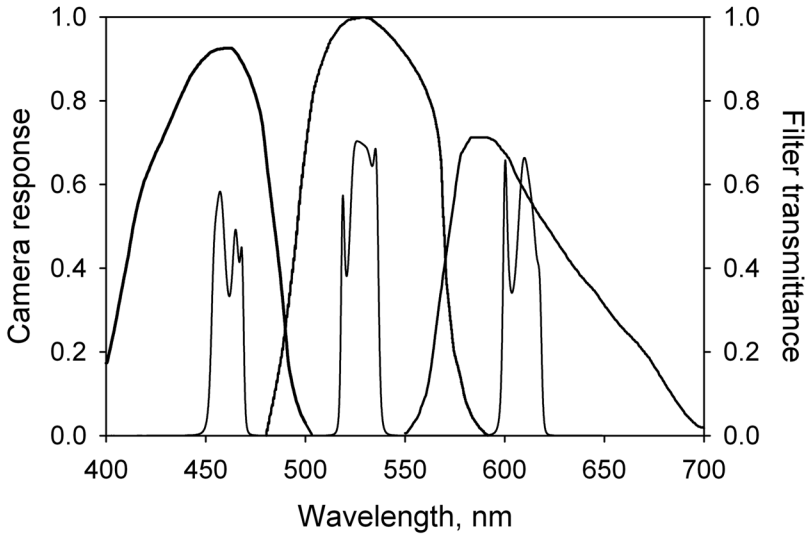

Fig. 2.

Spectral responses of the three CCDs in the Topcon TRC NW5SF retinal camera represented by the three broad bands. The narrower bands represent the transmittance characteristic of the triple-band filter. Its effect is to limit the wavelength response range of each CCD.

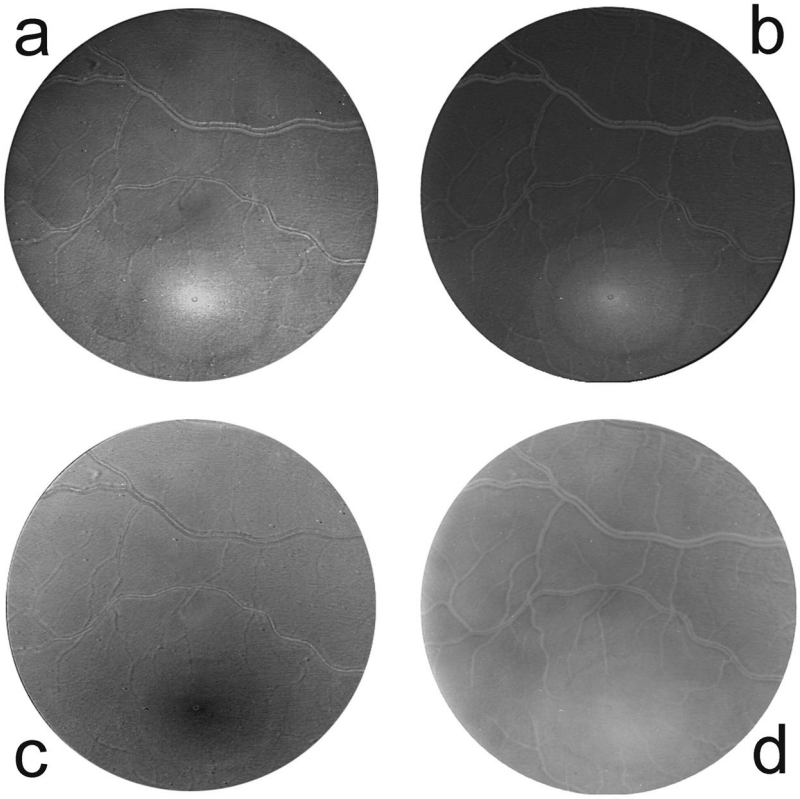

Fig. 3.

Relative optical density distributions of a) macular pigment at 460 nm, b) cone photopigment at 550 nm, c) rod photopigment at 505 nm, and d) melanin at 460 nm. The relative optical densities are represented by the pixel values in these images (i.e. higher optical density = brighter pixel). Thus the macular pigment (a) and cone photopigments (b) can be seen to peak in the fovea (lower center), the rod photopigments (c) dip to a minimum in the fovea, and melanin (d) is more broadly distributed.

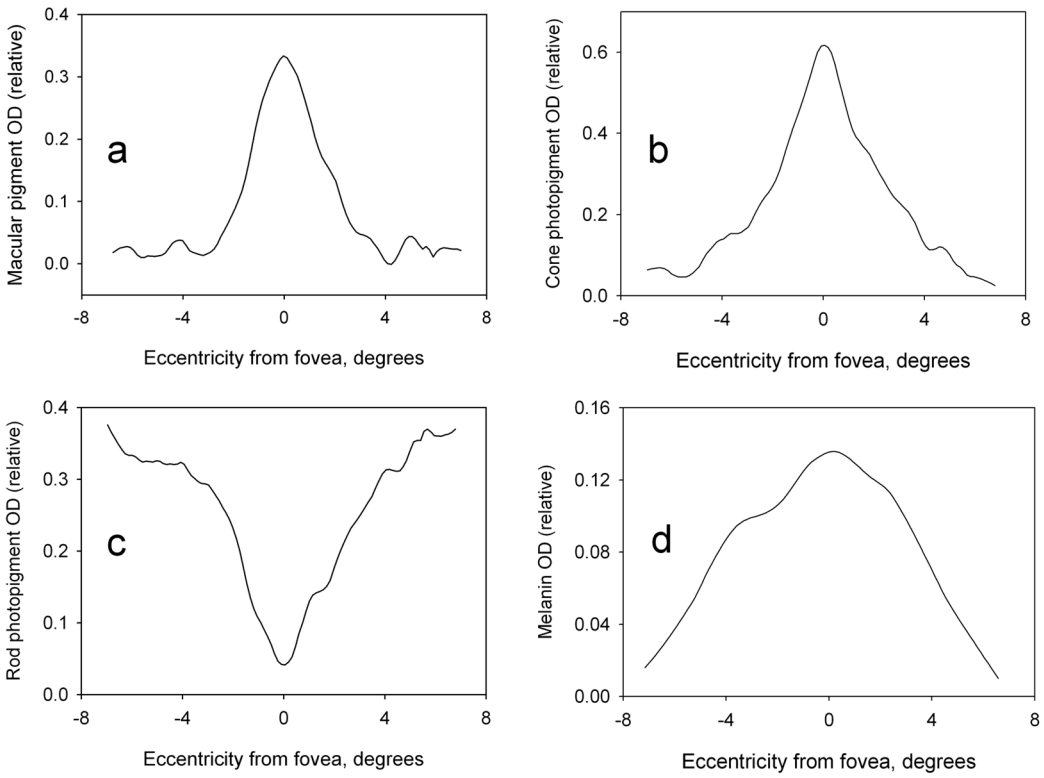

Fig. 4.

Horizontal line-scans through the foveal regions in Fig. 3. The scans provide quantitative measurements of the relative optical density distributions at 460 nm of a) macular pigment, b) cone photopigment, c) rod photopigment, and d) melanin along a horizontal meridian through the fovea.

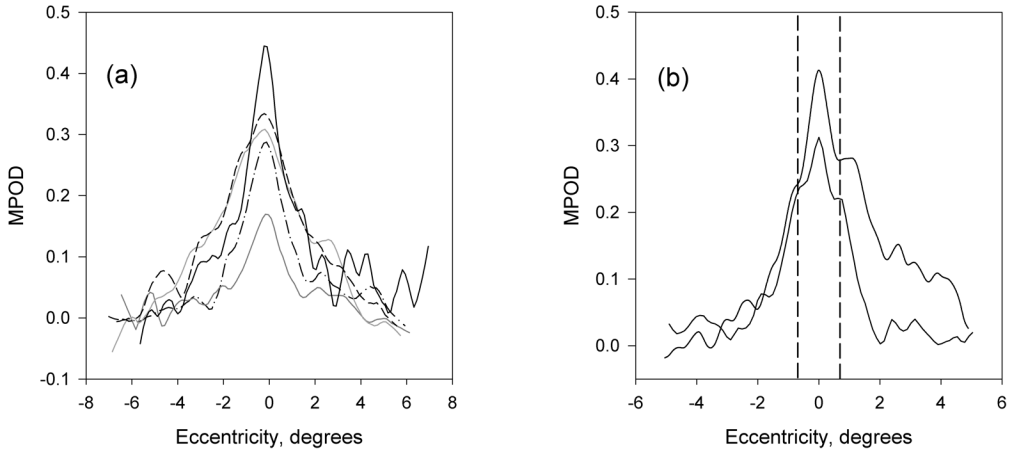

Fig. 5.

Macular pigment relative optical density distributions at 460 nm along a horizontal meridian through the fovea. a) Five subjects with reasonably monotonically decreasing macular pigment optical densities. b) Two subjects with subsidiary maxima/shoulders at ~ 0.7° eccentricity (vertical dashed lines), indicative of a ringlike feature of the macular pigment distribution.

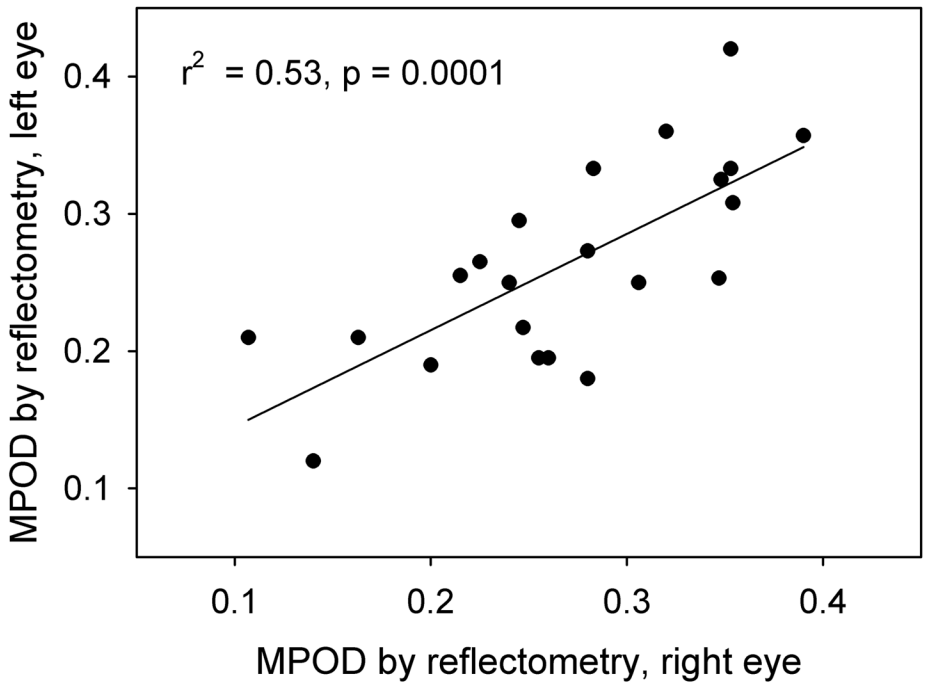

Fig. 6.
Comparison between peak macular pigment optical densities determined with the retinal camera in the left and right eyes of 22 subjects.

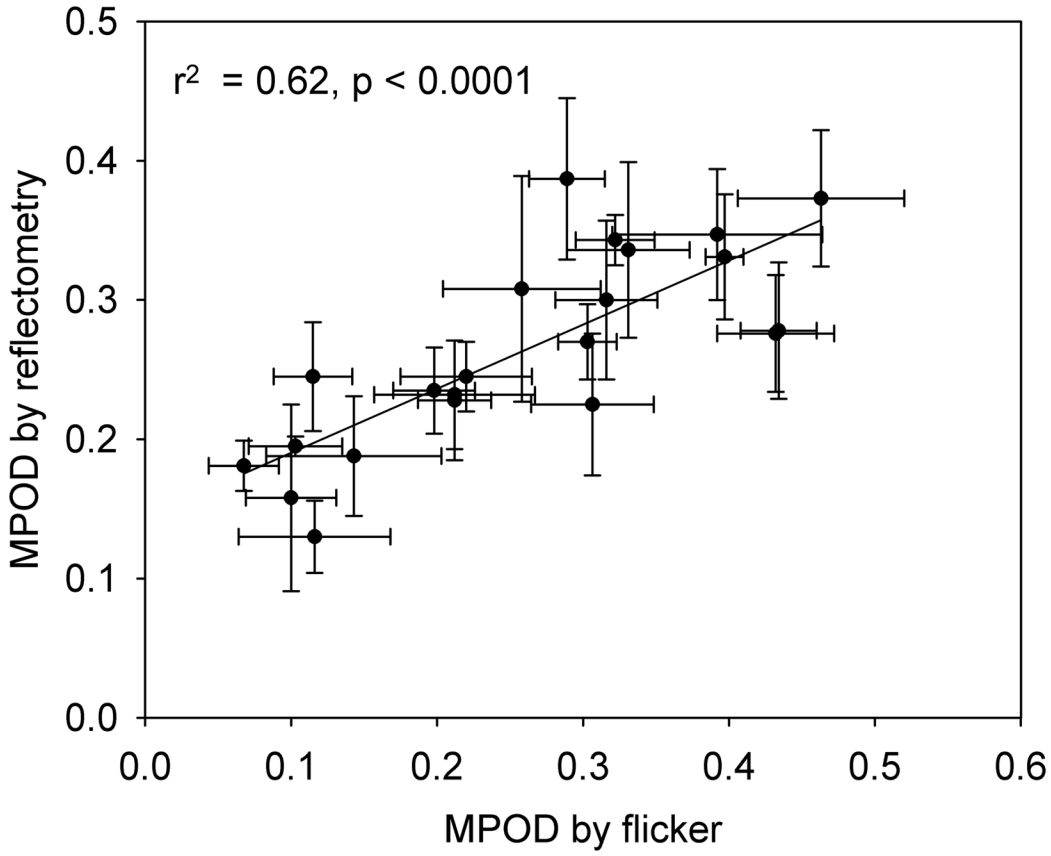

Fig. 7.

Comparison between peak macular pigment optical densities measured with the retinal camera and macular pigment optical densities obtained by heterochromatic flicker photometry for 22 subjects. For both procedures, data for left and right eyes are averaged. The error bars represent standard deviations.

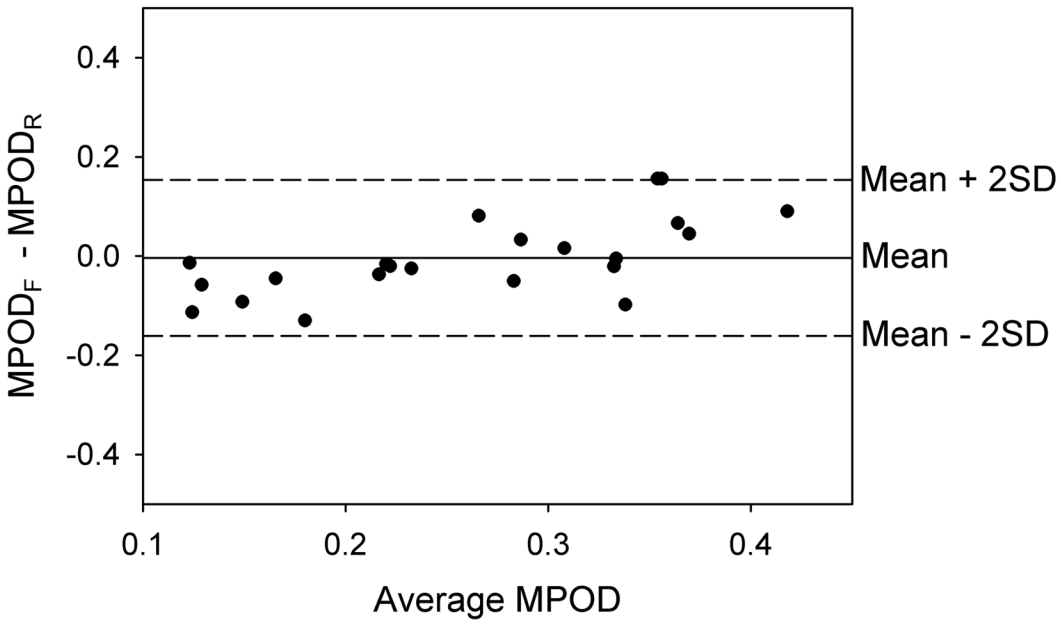

Fig. 8.

Bland-Altman plot for 22 subjects showing the difference between macular pigment optical densities obtained by HFP and reflectometry as a function of the mean value for the two methods. The solid horizontal line, representing the mean difference is very close to zero. All of the data points lie within 2 standard deviations of the mean (dashed horizontal lines).